Appl Nanosci (2015) 5:393–402
DOI 10.1007/s13204-014-0329-y

ORIGINAL ARTICLE

First-principles study of the interaction of hydrogen molecular on Na-adsorbed graphene

Nurapati Pantha · Kamal Belbase · Narayan Prasad Adhikari

Received: 3 May 2014 / Accepted: 8 June 2014 / Published online: 22 July 2014

Abstract We have performed density functional theory-based first-principles calculations to study the stability, geometrical structures, and electronic/magnetic properties of pure graphene, sodium (Na)-adsorbed graphene and also the adsorption properties of H_2-molecular ranging from one to five molecules on their preferred structures. Using the information of binding energy of Na at different adsorption sites of varying sized graphene supercell, it has been observed that hollow position is the most preferred site for Na adsorption, and the same in 3×3 supercell has been used for further calculations. The band structure and density of states calculations have been performed to study the electronic/magnetic properties of Na-atom graphene. On comparing adsorption energy per H_2-molecular in pure and Na-adsorbed graphene, we find that presence of Na atom, in general, enhances binding strength to H_2-moleculars.

Keywords Atom-adsorbed graphene · Hydrogen storage · Renewable energy · Density functional theory (DFT)

Introduction

Graphene is a two-dimensional layer of carbon atoms in honeycomb lattice structure, arranged with sp^2-hybridization (Geim and Novoselov 2007). With a number of wonderful properties, graphene has a long history (more than 60 years) of being studied first theoretically in 1947 (Wallace 1947) and later on experimentally in 2004 (Novoselov et al. 2004). Besides the attractive physical properties as a thin, strong and stretchable material (Geim 2009), graphene has interesting electronic/magnetic properties which enhances its potential use in academic and industrial world.

Graphene, its derivatives and other similar two-dimensional compounds have become frontier area of research activities, and also the materials of commercial interest in recent days (Medeiros et al. 2010; Johll et al. 2009; Thapa et al. 2011; Chan et al. 2008; Karki and Adhikari 2014; Ci et al. 2010; Kaloni et al. 2011; Park and Louie 2010; Kaloni et al. 2013; Esquinazi et al. 2003; Mukherjee and Kaloni 2012; Ugeda et al. 2010; Singh et al. 2013; Kaloni et al. 2014; Saha et al. 2009; Kaloni et al. 2012; Wu and Yang 2012; Dai et al. 2009; Choi and Jhi 2009). Graphene, hexagonal boron nitride (h-BN) and their doped structures have been studied by a number of research groups to see their potential applications in advanced electronics and optics (Ci et al. 2010; Mukherjee and Kaloni 2012; Singh et al. 2013). Also the multilayer graphene and other graphitic arrangements with electron donor/acceptor atoms, at varying concentrations, are covered to see their modified magnetism, and band structures (Kaloni et al. 2011, 2014, 2008; Park and Louie 2010; Kaloni et al. 2012; Ataca et al. 2008). The varying band gaps of these new materials and other carbon nanostructures include extensively a wide range of conductivity with all the potential applications in semiconductor (Mukherjee and Kaloni 2012; Kaloni et al. 2014), conductor (Ataca et al. 2008) to superconductor (Ugeda et al. 2010). The easily tunable structural stability, band structure and other electronic/magnetic properties, and also photonic and vibrational properties of graphene

Electronic supplementary material The online version of this article (doi:10.1007/s13204-014-0329-y) contains supplementary material, which is available to authorized users.

N. Pantha · K. Belbase · N. P. Adhikari (✉)
Central Department of Physics, Tribhuvan University, Kirtipur, Kathmandu, Nepal
e-mail: npadhikari@gmail.com

have been achieved through a number of techniques like: via vacancies (Kaloni et al. 2013; Ugeda et al. 2010; Singh et al. 2013; Kaloni et al. 2012), atomic/molecular doping (Medeiros et al. 2010; Johll et al. 2009; Thapa et al. 2011; Chan et al. 2008; Karki and Adhikari 2014; Saha et al. 2009; Wu and Yang 2012), functionalization (Wood et al. 2012; Ulman et al. 2014), irradiation (Esquinazi et al. 2003) and external fields (Park and Louie 2010). The modified compounds carry potential applications over many dimensions like in electronics (Geim 2009; Novoselov et al. 2005, 2007), spintronics (Palacios et al. 2008; Ding et al. 2011), chemical sensors (Saha et al. 2009), and energy storage (Pumera 2011). Graphene with the adsorption of relevant metal atoms, clusters and other functional groups as impurities have been seriously considered and studied as substrates for gaseous adsorption (Wu and Yang 2012), including energy carrying gases methane and hydrogen (Wood et al. 2012; Ulman et al. 2014).

Hydrogen, either in gaseous form or as a component of abundant compounds like water and hydrocarbons, is a widely available energy resource in the Earth and extra-terrestrial planets. As hydrogen releases only the water vapour when it burns, it is considered as one of the clean and green sources of energy. In spite of having many advantages to be a potential gas for future energy carrier, user friendly storage and transportation have become one of the major challenges. There are a number of traditional techniques which have been practiced to store natural gases and hydrogen, like in tanks under high pressure (Compressed natural gases, CNG) (Burchell and Rogers 2000; Duren et al. 2004) and in liquid form at low temperature (Liquefied natural Gases, LNGs) (Nakanishi and Reid 1971) or in chemical hydrides (Orimo et al. 2007). The techniques, however, are not user friendly due to weight, space and economy concerned perspectives and also they display the risk of leakage and explosion (Chen et al. 1999). Adsorption of hydrogen in different porous materials (Ma et al. 2008) and carbon nanomaterials including activated carbons is some of the highly searched techniques in recent time (Pan et al. 2008). It has been reported that an appreciable amount of hydrogen could be stored at low temperature and the continuous development is going on to develop the devices which are suitable to store hydrogen at operating conditions. Among the carbon nanotubes and graphene allotropes as substrates for hydrogen adsorption, adatoms including alkali elements have performed catalytic effect in dissociating the H_2 molecule, promoting atomic adsorption and enhancing binding strength at moderate temperature and ambient pressure (Kwon 2010; Chen et al. 2008; Chandrakumar and Ghosh 2008). The United State's department of energy (US, DOE) has set targets of about 6 wt% (Durgun et al. 2008) and adsorption energy range (0.2–0.7 eV) (Zhou and Willians 2011) for hydrogen storage in practical applications like vehicular transportation. Approaching towards these goals by designing the proper substrate will explore interesting scientific and commercial implications.

The adsorption of alkali metal atoms on graphitic materials has been widely studied to see the interaction between them (Medeiros et al. 2010; Liu et al. 2011). Being as electron donor atoms, electronic charge transfers from adsorbed alkali atoms (Li, Na and K) to graphene, which causes change in band structure and neutrality of the new materials (Mukherjee and Kaloni 2012). The properties of atom-adsorbed graphene can also be tuned using mechanical strain (Zhou et al. 2010). Among the alkali metal atoms, Li with its light weight has been previously tested to metalize graphene, which enhances hydrogen storage capacity up to 12.8 wt% (Ataca et al. 2008). Having similar electronic properties and slightly higher molecular weight, Na could be a good option for catalyzing graphene to store H_2-moleculars. However, in our best knowledge, this element neither as an isolated atom nor as a cluster in carbon nanostructures has been checked for enhancing gaseous adsorption. In the present work, we first see the nature of interaction between the Na atom with monolayer graphene and then Na-graphene system is used to study its binding strength for H_2-moleculars.

Computational details

Density functional theory (DFT)-based first-principles calculations (Hohenberg and Kohn 1964; Kohn and Sahm 1965) are carried out to investigate the structural stability and electronic/magnetic properties of graphene and single sodium atom added graphene. The optimized geometry of 3×3 Na-added graphene, based on compromise between the size effect and the computational cost, is then used as substrate to study the adsorption behavior of a number of H_2-molecular. The calculations are performed by incorporating van der Waals (vdW) interactions (Klimes and Michaelides 2012) via London dispersion effects in DFT-D2 approach, implemented with the quantum ESPRESSO package (Giannozzi et al. 2009). The algorithm has used Rappe–Rabe–Kaxiras–Joannopoulos (RRKJ) model of ultrasoft pseudopotential to account the interaction between the ion cores and valence electrons and generalized gradient approximation (GGA) formalism to treat the electronic exchange and correlation effects, as described by Perdew–Burke–Ernzerhof (PBE) (Perdew et al. 1996), for all the species (C, Na, H). The semi-core states: $2p3s$ of sodium, $1s$ of hydrogen and $2s2p$ of carbon atoms are treated explicitly as valence in the pseudopotential description of the corresponding atoms. The inner cores for carbon and sodium, on the other hands, are included as ion

cores by the corresponding pseudo potentials Quantum (2014).

A hexagonal unit cell with the basis of two atoms in honeycomb lattice structure was initially constructed using experimental value (Castro Neto et al. 2006, 2009). The structure was then optimized with respect to lattice parameter (a), cut off energy of the plane waves and the number of k-points along x and y axes, respectively. Based on these convergence tests, a plane wave basis set with the kinetic energy cutoff 35 Ry is used for the expansion of the ground state electronic wave function. The plane waves are chosen to have a periodicity compatible with the periodic boundary conditions of the simulating cell. In case of lattice constant, we have used the calculated value (2.46 Å) which comes to agree with the experimental value for the planner sides of the unit cell, whereas the dimension along z-direction is kept large enough (20 Å) to avoid the interaction between the graphene layers and also to provide the space for upcoming hydrogen adsorption calculations. Similarly, we have used 15 × 15 × 1 mesh of k-points from convergence test for the unit cell calculations (Fig. 1).

The Na-adsorbed graphene system is modeled using single Na atom in the 2 × 2, 3 × 3 and 4 × 4 supercell of graphene containing 8, 18, and 32 number of carbon atoms. In this work, the adsorption of sodium on graphene is performed at three different occupation sites: the Top (T) site directly above the carbon atom, the Hollow (H) site at the center of hexagon and the bridge (B) site at the midpoint of the C–C bond (Fig. 2). For each adsorption site of the adatom-graphene system, the foreign atom (Na) and C atoms on graphene are relaxed in all x, y and z directions. To estimate the binding energy of Na, the calculations for the isolated Na, isolated graphene and Na-adsorbed graphene system are performed in same-sized graphene supercell.

During the process of calculations, we have first performed the relaxation of initial geometries to obtain the optimized structures. The systems thus calculated are

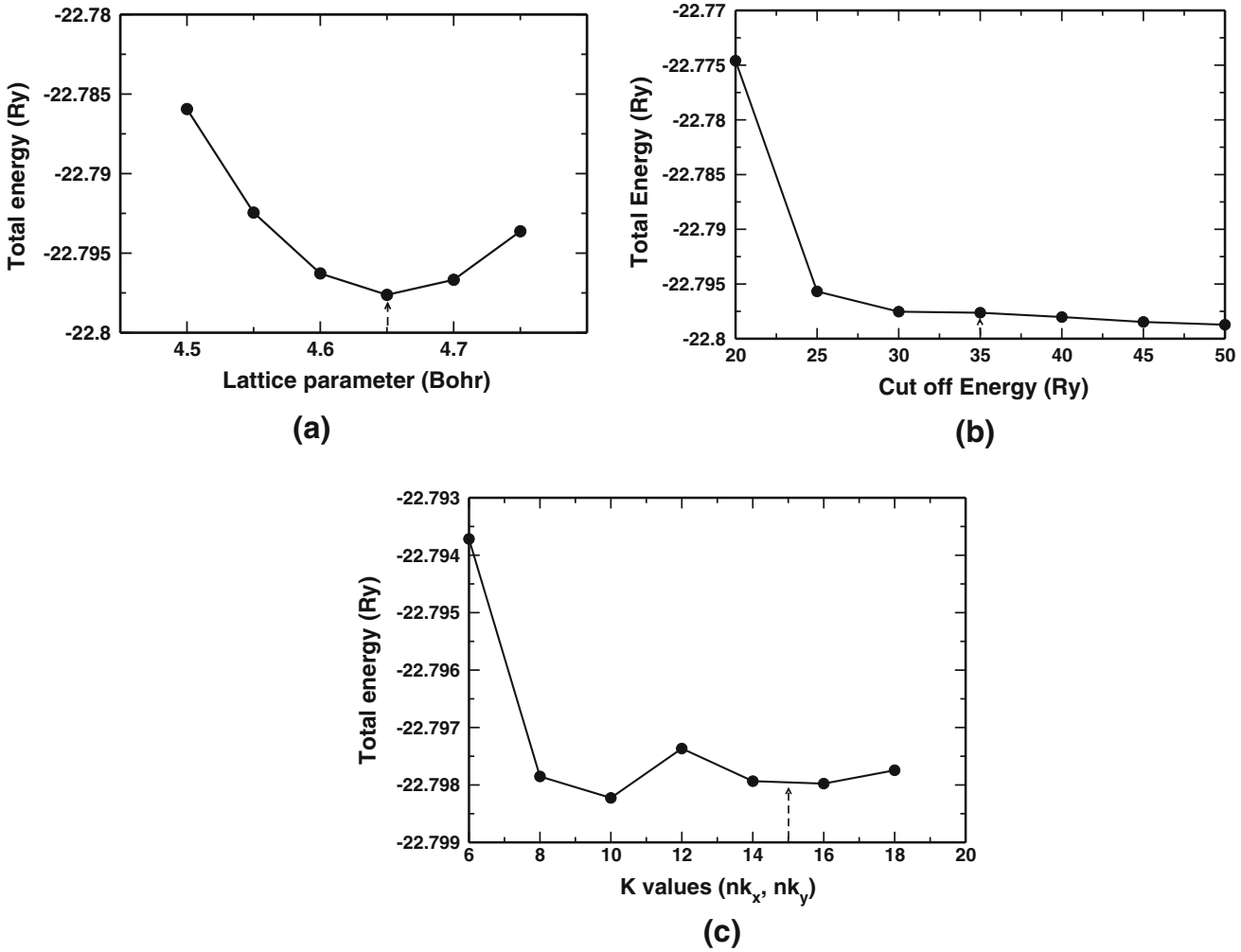

Fig. 1 The convergence of total energy with respect to the lattice parameter (**a**), cut off energy (**b**) and k-points (**c**)

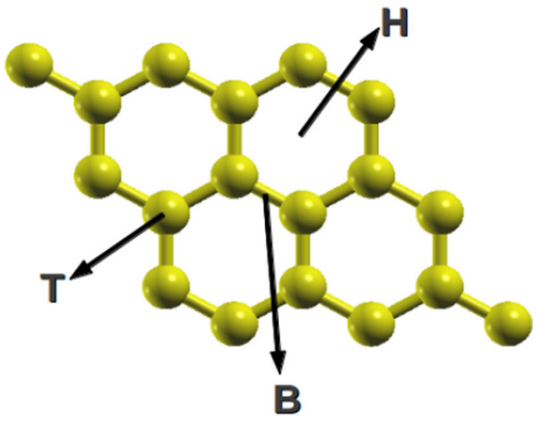

Fig. 2 Three occupation sites top (T), bridge (B) and hollow (H) of the graphene sheet are shown

allowed fully to relax using BFGS (Broyden–Fletcher–Goldfarb–Shanno) scheme until the total energy changes between two consecutive self-consistent field steps are less than 10^{-4} Ry and force acting is less than 10^{-3} Ry/Bohr. The first Brillouin zone of graphene is sampled in the reciprocal space using the Monkhorst–Pack scheme with an appropriate number of k-points, as described by the convergence test. Smearing was incorporated to aid the convergence. We have used 'Marzarri–vanderbilt' method (Marzari et al. 1999) or cold smearing with a small Gaussian spread of 0.001 Ry. Furthermore, we have chosen 'david' diagonalization method with the mixing factor 0.6 for self consistency. Spin polarized calculations are accommodated to study the magnetic properties of the systems. For the density of states (DOS) calculations of pure graphene and sodium-adsorbed graphene systems, we have used 3×3 supercell of graphene with a denser mesh of $(15 \times 15 \times 1)$ k-points.

We have also investigated the stability of hydrogen adsorption on sodium added graphene system. As a first step, H_2-molecular was relaxed on similar box of 3×3 graphene supercell and then defined its optimized geometry accordingly. The bond length of H_2 molecule calculated in this way has been found as 0.75 Å which agrees with the previously reported value (Arellano et al. 2012). Due to the periodicity of the crystal, the distance between two H_2-moleculars of nearest supercells becomes equal to the cell dimension (i.e., 9.299 Bohr) which is large enough compared to the molecular bond length of H_2 (i.e., 1.418 Bohr). This situation ensures that there is no interaction between two H_2-moleculars located at adjacent supercells.

Results and discussion

In the present work, we study the adsorption of single sodium atom on three different occupation sites of 2×2, 3×3 and 4×4 supercells of pure graphene. Furthermore, we extend our work to study the adsorption of H_2-moleculars on pure graphene and Na-adsorbed graphene.

Adsorption of sodium atom on graphene

We discuss structural, electronic and magnetic properties of pure and sodium added graphene in this section.

The binding energy of sodium atom on graphene sheet is calculated using relation,

$$\Delta E = E_{\mathrm{Na}} + E_{\mathrm{G}} - E_{\mathrm{G+Na}} \quad (1)$$

where E_{Na}, E_{G} and $E_{\mathrm{G+Na}}$ are the ground state energies of sodium atom, pure graphene and sodium-adsorbed graphene systems in the fixed supercells, respectively. The positive binding energy from Eq. (1) indicates stable configurations. We have defined the most preferred sites/geometries of the systems for 2×2, 3×3, and 4×4 supercells separately by taking information of the largest binding energy values from these calculations.

The adatom height (h) is defined as the difference in z coordinate of the Na and an average of z coordinates of the C atoms in graphene layer. We have also calculated the distance (d_{Ac}) between the adsorbed atom and its nearest carbon atom. The adsorption of sodium on graphene produces a small distortion which is quantified by computing the maximum deviation in z direction of C atoms in graphene layer from their average initial position. This distortion of the graphene layer upon the adsorption of a foreign atom (Na in this case) is also calculated in terms of change in dihedral angles.

The binding energy of sodium atom on hexagonal 2×2 graphene supercell, containing 8 carbon atoms, has been calculated as -0.29, -0.38, -0.39 eV on H, B, and T sites, respectively. This signifies that Na-adsorbed graphene in 2×2 supercell is less stable than its constituent systems (the pristine graphene and isolated Na atom), which agrees with the previously reported results for two-atom unit cell (Medeiros et al. 2010).

The supercells of larger size are more favorable for the adsorption of Na atom. Table 1 presents the binding energy values, the equilibrium distances from the average graphene sheet (h), the distance of adatom (Na) from the nearest carbon atom (d_{AC}) of graphene and also the distortion of the graphene sheet d_{GC} in 3×3 supercell. The table quantifies binding energies of sodium atom at the hollow (H), bridge (B), and top (T) sites as 0.45, 0.31 and 0.33 eV, respectively. The values imply that sodium atom is bound to all the tested sites of the graphene sheet and the H site is the most favored one among them. This conclusion agrees with the previously reported results (Chan et al. 2008; Oli et al. 2013). The equilibrium distance of sodium atom from the surface of graphene sheet is found to be 2.32 Å for H

Table 1 The adsorption energy of sodium atom ΔE, its height from graphene sheet (h), the distance of the nearest carbon atom of the sheet (d_{AC}), and the distortion observed in 3 × 3 graphene sheet due to adsorption of sodium atom (d_{GC}) are listed in this table

Atom	site	ΔE (eV)	h (Å)	d_{AC} (Å)	d_{GC} (10^{-2} Å)
Na	H	0.45	2.32	2.72	0.94
	B	0.31	2.42	2.57	−0.08
	T	0.33	2.41	2.48	−0.53

site, 2.42 Å for B site, and 2.41 Å for T site. The smallest equilibrium distance at H site signifies that there exists the strongest interaction between the sodium atom and carbon atoms of this site compared to those at B and T sites. The distortion produced by sodium is found only about 0.009 Å for hollow (H) site. The magnitude, however, is not significant (noticeable distortion is defined for ≥ 0.07 Å (Chan et al. 2008)) and this is true for bridge and top sites as well. Since the distortion in the graphene sheet (3 × 3 supercell) is not significant, C−C bonds near the Na atom retain their sp^2 character and do not rehybridize significantly with any adsorbed atom orbitals.

In the case of 4 × 4 supercell, the binding energy of sodium atom at hollow site is found to be 0.78 eV. This value is significantly higher than that for 3 × 3 supercell at the same (H) site (0.45 eV). It has been found that the binding energy of adsorbed metal atoms is size dependent and gets almost constant value beyond certain number of C atoms in graphene. Oli et al. (2013) have reported rapid change in binding energy of alkali metal atoms (Li, Na and K) on graphene before reaching its saturation size, i.e., 48 number of carbon atoms. The quantities revealed by the authors for Na in passivated graphene structure of 16 carbon atoms of $C_{16}H_{10}$ and 30 carbon atoms of $C_{30}H_{14}$ are 0.32 eV and 0.72 eV, which are reasonably close to the present work of 18 (3 × 3 supercell) and 32 (4 × 4 supercell) atoms of graphene sheets, respectively (Oli et al. 2013). Ding et al. (2011), on the other hand, have reported different trends of size dependency of binding energy for different atoms, while varying graphene supercell from 3 × 3 to 4 × 4. The authors find binding energy difference in between 3 × 3 and 4 × 4 supercells for the elements of transition metals moving from Sc to Cu, in general, in decreasing trend. In separate calculations, we have observed very slight change in binding energy of Pt in 4 × 4 graphene supercell with respect to that in 3 × 3 graphene, while it is noticeable in between 2 × 2 and 3 × 3 (Lamichhane et al. 2014). It can, therefore, be concluded that size dependency of binding energy and also the saturation size of graphene depend on the chemistry of elements and usually higher for monovalent atoms.

The equilibrium distance between the sodium atom and graphene sheet in 4 × 4 supercell, $h = 2.25$ Å, is lower than that in smaller supercells. Also the distance of the nearest carbon atom at hexagonal site from the sodium, d_{AC}, is found to be 2.69 Å. Both the geometrical parameters, h and d_{AC}, from the present results come in good agreement with the previous work performed by Chan et al. (2008) where the values are reported as 2.28 and 2.70 Å respectively, in the same-size (4 × 4) supercell. Sodium atom produces a small distortion, 0.008 Å, to the graphene sheet of 4 × 4 supercell as well. The distortion falls in the similar range to that of the 3 × 3 supercell of graphene system with slightly higher value in the smaller size. The small positive distortion implies that graphene sheet gently moves towards the sodium atom (upwards), due to interaction between them.

The density of states (DOS) and the band structure calculations of 3 × 3 pure and Na-adsorbed-graphene systems disclose the changes in electronic/magnetic properties of the systems, due to presence of Na, over the pure graphene.

The DOS for spin up and spin down states with reference to Fermi level (represented by the vertical dotted line) are shown in Figs. 3, and 4. In case of pure graphene (Fig. 3), the Fermi level lies at −2.35 eV and the DOS for spin up and spin down are seen symmetrical. Dirac point, where DOS is zero, lies exactly at the Fermi level. This symmetry of DOS about the Fermi level implies that pure graphene is non-magnetic. However, Dirac point shifts below the Fermi level and also the symmetry of DOS is broken with the extra peaks at/near the Fermi level when Na is adsorbed in graphene (Fig. 4). The shifting of Dirac point below the Fermi-level has also been discussed in Mukherjee and Kaloni (2012) for nitrogen-doped (N-doped) graphene system, where N contributes as an electron donor as similar to Na in the present work. Figure 4 also indicates its modified conductivity with reference to zero-band gap pristine graphene, which is consistent with the Medeiros et al. (2010). The breaking of symmetry, on the other hand, introduces the magnetic behavior. In case of

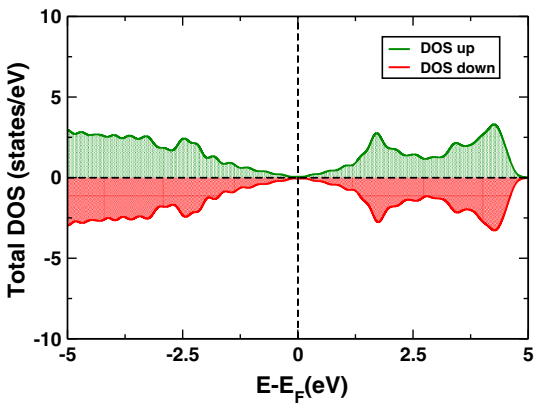

Fig. 3 Density of states (DOS) of pure graphene

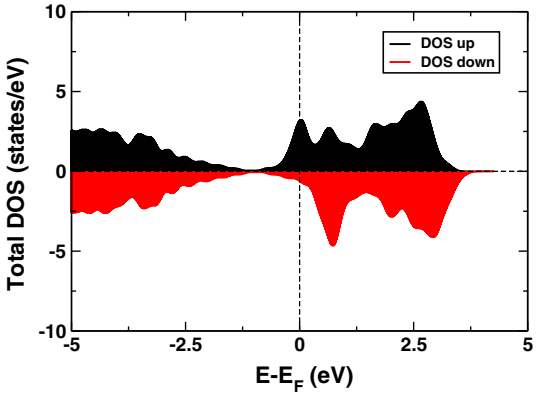

Fig. 4 Density of states (DOS) of Na-adsorbed graphene

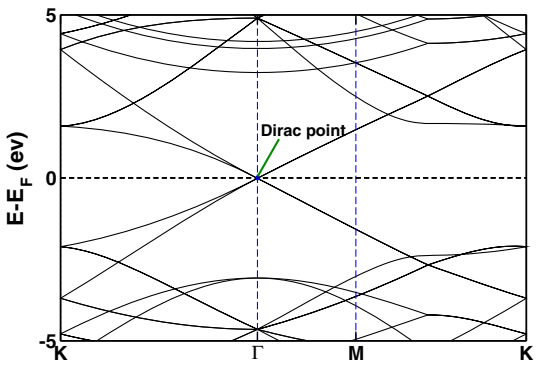

Fig. 5 The band structure of the pure graphene

3×3 supercell of graphene, the value of magnetization is 0.08 μ_B where as that for 4×4 supercell is 0.24 μ_B. The total magnetization of 4×4 supercell from this work agrees well with the previously reported value 0.27 μ_B (Chan et al. 2008). However, these values of magnetic moments for Na-graphene systems are lower than that for isolated sodium atom estimated theoretically (using electronic configurations) and computationally (present work) (1.0 μ_B). We believe that this reduction in magnetization could be due to partial transfer of electronic charge from Na to the graphene.

We have performed the band structure calculations by defining high symmetry points (i.e., K, Γ and M) on the edges of irreducible Brillouin zone in reciprocal space. In this case, we have taken 100 k-points along the specific direction of irreducible Brillouin zone to obtain the fine band structure. Figures 5 and 6 represent the band structure of pure graphene and Na-graphene systems, respectively.

Graphene is a single atomic layer of graphite where the carbon atoms condense in a honeycomb lattice due to their sp^2 hybridization of $2s$, $2p_x$, and $2p_y$ orbitals of three valence electrons out of four valence electrons. The mixing of the 2s and two 2p orbitals gives the planar sp^2 hybridization. The electrons involved in sp^2 hybridization are

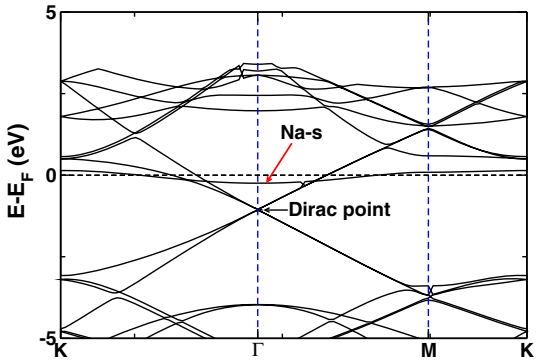

Fig. 6 The bands structure of Na-graphene system. The *red arrow* shows the s-orbital contribution of Na atom

localized and form σ bonds. These electrons do not contribute to the transport phenomenon. The fourth electron, perpendicular to the plane of graphene sheet, occupies the $2p_z$ orbital and forms the π-bond with $2p_z$ electron of neighboring carbon atom (Novoselov et al. 2005). These electrons forming π-bond, however, are delocalized over the entire lattice and have higher energy than the electrons that form the σ-bonds. Most of the interesting properties of graphene arise due to these delocalized π-electrons (Novoselov et al. 2007). The bands above and below the Fermi level are referred to π^* and π bands, respectively. In case of pure graphene, these conical π bands meet at the Fermi level and the band gap formed by them becomes zero (Fig. 5). The pure graphene thus is also known as zero band gap semiconductor. The meeting point of the conical bands (also known as Dirac point) and the conical region around the Dirac point (also known as Dirac cone) are the special properties of graphene and they are successfully produced in our calculations.

The band structure of Na-graphene system, on the other hands, shows that Dirac point shifts below the Fermi level by 1.084 eV (Fig. 6), similar to the results described by Liu et al. (2011). When the electron donor Na atom is adsorbed on graphene, a fraction of electronic charge transfers from the sodium atom towards the carbons of graphene. Since the π band of the graphene is already occupied, the transferred charge from sodium moves towards the π^* band (Medeiros et al. 2010). If we compare the Fermi level of pure graphene and Na-adatom graphene, it lies at -2.346 eV in the former case and rises to -0.695 eV after the adsorption of Na atom. It means that the Fermi level shifts by 1.651 eV towards the conduction band (upwards) due to Na contribution. Furthermore, an extra band nearby Fermi level is clearly seen and marked as *s* orbital contribution of Na in Fig. 6, which is similar to Li contribution on graphene reported in Kaloni et al. (2013). The conduction band and valence band overlap in sodium-added graphene, and this suggests that the new material is conductor.

Adsorption of H_2-molecular/s

In this section, we discuss the geometry and the stability of adsorption of H_2-molecular/s on pure and sodium-adsorbed graphene systems.

Adsorption of H_2-molecular on the pure graphene

We have considered a number of samples to study the interaction between pure graphene sheet and single H_2-molecular in perpendicular and parallel orientations at different positions of 3×3 supercell of graphene. The perpendicular configurations, H_2 molecule perpendicular to the graphene plane at top, bridge and hollow sites, are shown in Figs. 7, 8, and 9, respectively. Figure 10, on the other hand, defines the parallel configuration of H_2 at hollow position of the graphene.

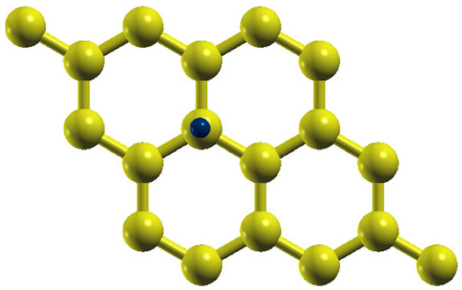

Fig. 7 H_2 molecule perpendicular to the carbon atom (top site)

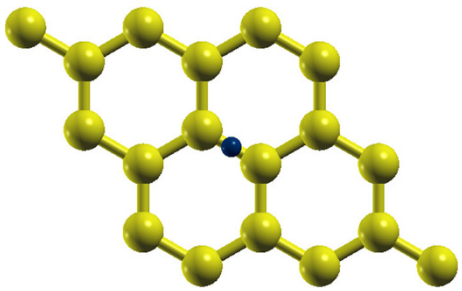

Fig. 8 H_2 molecule perpendicular to the carbon–carbon bond (bridge site)

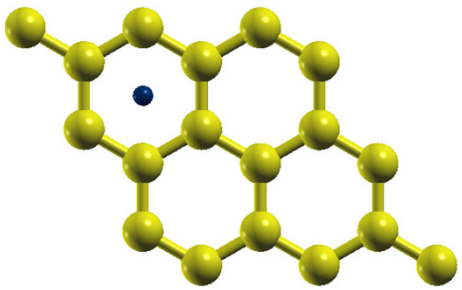

Fig. 9 H_2 molecule perpendicular to the center of hexagonal ring of carbon atoms (hollow site)

The adsorption/binding energy (ΔE) of H_2 molecule, will be referred as adsorption energy hereby, is calculated from the optimized geometry of H_2-graphene system using equation

$$\Delta E = E_G + E_{H_2} - E_{G+H_2} \quad (2)$$

with appropriate replacements of combined and individual components of the system. In this case, E_G, E_{H_2}, and E_{G+H_2} are the ground state energy of pure graphene, H_2-molecular, and H_2-graphene (combined) systems, respectively. The values are calculated using same-sized supercell of graphene. The magnitudes of adsorption energy of H_2 molecule and its distance from the graphene plane are presented in Table 2.

Table 2 shows that the adsorption energy is maximum and the equilibrium distance is minimum for H_2 molecular of its perpendicular configuration at hollow (H) site of graphene. This confirms that H_2 molecular perpendicular to the hexagonal ring is most stable than any other configurations. The calculated values of adsorption energy of H_2 molecular from the present work (61–69 meV) in the pure graphene sheet lie within the range of previously reported values (55–80 meV) (Kwon 2010). Small adsorption energy for single hydrogen adsorption could be because of very strong intra-molecular H–H bond, extremely small induced dipole moment, and the chemically inert nature of the our system (i.e., graphene). The small adsorption causes the weak binding of H_2 mainly due to van der Waals

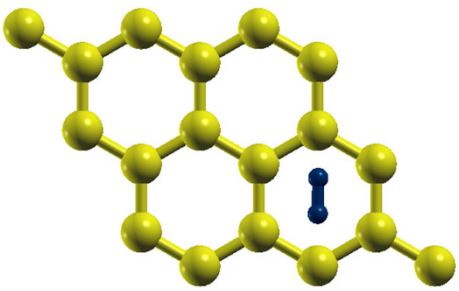

Fig. 10 H_2 molecule parallel to the hexagonal ring of carbon atoms

Table 2 The table quantifies the adsorption energy of single H_2 molecule when adsorbed in perpendicular and parallel configurations at bridge (B), top (T) and hollow (H) positions of the graphene sheets (ΔE). The symbol 'h' represents the equilibrium distance of H_2 molecular, measured from the lower atom of H_2 in perpendicular case, from the graphene sheet

Position of H_2	Binding energy ΔE (meV)	h (Å)
Perpendicular at B	62.9	2.67
Perpendicular at T	61.9	2.72
Perpendicular at H	68.6	2.48
Parallel at H	66.2	2.82

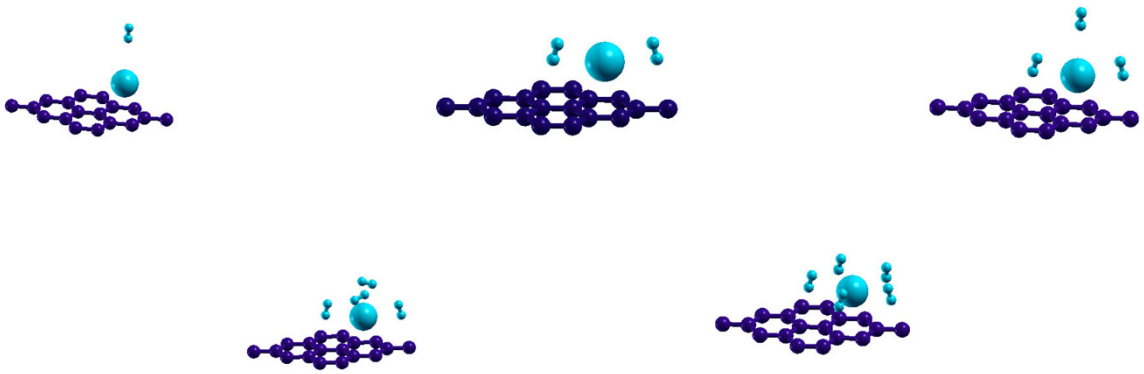

Fig. 11 Adsorption of a varying number of H_2-molecular on Na-adsorbed graphene system

Table 3 The adsorption energy of H_2-moleculars (E_{NH_2}) and adsorption energy per H_2-molecular (E_{H_2}) are listed

Number of H_2	E_{NH_2} (eV)	E_{H_2} (eV)
1	0.023	0.023
2	0.174	0.087
3	0.405	0.135
4	0.628	0.157
5	0.960	0.192

interaction, and can be easily taken out from system, even at low temperature.

Adsorption of H_2-molecular/s on the sodium-adsorbed graphene

The adsorption of varying number of H_2-moleculars (one to five) has been tested on sodium-adsorbed 3 × 3 graphene supercell, and the adsorption energy of the same is computed by

$$\Delta E = E_{\mathrm{G+Na}} + NE_{\mathrm{H_2}} - E_{\mathrm{G+Na+H_2}} \quad (3)$$

where $E_{\mathrm{G+Na+H_2}}$ is the ground state energy of the graphene supercell after adsorbing sodium atom and H_2-moleculars. Similarly, $E_{\mathrm{G+Na}}$ and $E_{\mathrm{H_2}}$ are the ground state energies of sodium-adsorbed graphene and molecular hydrogen, respectively. The number of H_2-moleculars is represented by N in the equation. The positive adsorption energy signifies that H_2-molecular bounds to the adatom-graphene system. The binding energy per H_2-molecular has been further calculated by,

B.E. per H_2-molecular = $\frac{\Delta E}{N}$

Figure 11 shows the optimized structures of hydrogen–sodium–graphene systems with a varying number of H_2-molecular.

Table 3 shows that the adsorption energy of H_2 molecular as well as adsorption energy per H_2-molecular increases continuously as we increase the number of molecules in the system. If we compare the adsorption energy per H_2 molecular with and without adatom in graphene supercell, it can be found that presence of Na enhances the binding strength except for N = 1. The adsorption energy per H_2 molecular ranges from 0.023 to 0.192 eV/H_2 for the adsorption of one to five numbers of H_2 molecular (Fig. 12). This range of adsorption energy comes in good agreement with the previously reported average binding energy of hydrogen, 0.09 to 0.22 eV for one to four molecules, in the Lithium-adsorbed graphene system (Ataca et al. 2008).

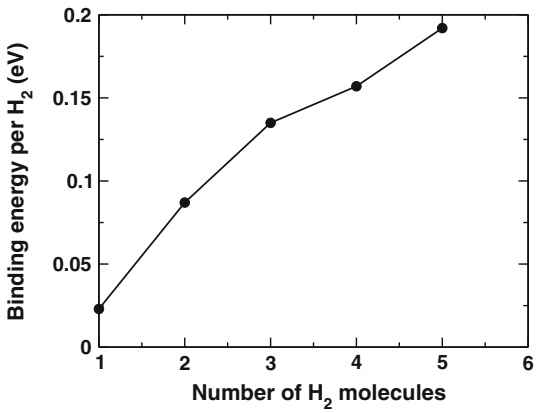

Fig. 12 The binding energy per H_2-molecular is in increasing order up to 5 H_2 molecular

Figure 12 shows that the adsorption energy per H_2-molecular increases and attains the maximum value (0.192 eV) as we increase the number of H_2-molecular from one to five. The maximum value (0.192 eV/H_2) approaches nearby one of the goals set by DOE, 0.2–0.7 eV for the practical applications (Zhou and Willians 2011) . However, this increasing pattern is seen dissimilar with our calculations of hydrogen adsorption in other metallic atom adsorbed-graphene (Pd/Pt-graphene) systems. The reason could be because of different structural/electronic structure of sodium compared to other atoms. We believe that further analysis of charge distribution before and after the

adsorption of gaseous molecules will explore the causes beyond these results.

Graphene and carbon nanomaterials have been considered as porous materials/substrates for the storage of energy carrying gases via adsorption at operating conditions. Similar to the previously accepted results, our calculations have found low adsorption energy of H_2 in pure graphene. However, the binding strength is enhanced significantly for 2–5 numbers of H_2-molecular in Na-adsorbed graphene. The content of hydrogen in the proposed system can also be analyzed on the basis of its presence by weight. For 5 molecular of hydrogen, the maximum number of molecules adsorbed in our calculations reaches 4.02 wt % (weight percentage) which is progressive towards the DOE (Department of Energy) target (around 6 wt %) for the practical applications (Durgun et al. 2008).

Conclusions

The structural and electronic properties of pure graphene and Na-graphene systems are studied. The binding energy values for Na at different sites suggest that the hollow site is the most favorable position for the adsorption of sodium atom on graphene sheet. The band structure and DOS calculations of the pure graphene find zero band gap and non-magnetic nature, which are consistent with the previously established facts. In case of sodium-adsorbed graphene system, the conduction band and valence band are overlapped. DOS are not symmetrical, which indicates that the system is magnetic, and the calculations find magnetic moment 0.24 μ_B for Na in 4×4 graphene supercell.

We have also performed the adsorption of H_2-molecular on pure graphene sheet and sodium-adsorbed graphene system. The present study reveals that the adsorption energy per H_2-molecular is enhanced due to the presence of Na atom and reaches 0.192 eV in case of Na-adsorbed graphene compared to its value 0.068 eV in pure graphene. The hydrogen storage capacity of Na-adsorbed graphene for the adsorption of five H_2-molecular has been calculated as 4.02 wt % (weight percentage), which is progressive towards the DOE (Department of Energy) target (around 6 wt %) for the practical applications.

Acknowledgments We acknowledge the partial support from The Abdus Salam International Center for Theoretical Physics (ICTP) through office of external activities within NET-56 project. We also extend our gratitude to S. Narasimhan and K. Ulman for their valuable suggestions and inspiration to work in this area. N. Pantha acknowledges to Nepal Academy of science and Technology (NAST), Nepal, for its partial financial support. We also acknowledge re-viewer's feedback for the improvement of this manuscript.

References

Arellano JS, Molina LM, Rubio A, Lopez MJ, Alonso JA (2012) Interaction of molecular and atomic hydrogen with (5,5) and (6,6) single-wall carbon nanotubes. J Chem Phys 117:2281

Ataca C, Aktürk E, Ciraci S, Ustunel H (2008) High-capacity hydrogen storage by metallized graphene. Appl Phys Lett 93:043123

Burchell T, Rogers M (2000) Low pressure storage of natural gas for vehicular applications. SAE Tech. Pap. Ser. 2000–01-2205

Castro Neto AH, Guinea F, Peres NMR (2006) Drawing conclusions from graphene. Phys World 19:33

Castro Neto AH, Guinea F, Peres NMR, Novoselov KS, Geim AK (2009) The electronic properties of graphene. Rev Mod Phys 81:109

Chan KT, Neaton JB, Cohen ML (2008) First-principles study of metal adatom adsorption on graphene. Phys Rev B 77:235430

Chandrakumar KRS, Ghosh SK (2008) Alkali-metal-induced enhancement of hydrogen adsorption in C60 fullerene: an ab initio study. Nano Lett 8:13

Chen P, Wu X, Lin J, Tan KL (1999) High H_2 uptake by alkali-doped carbon nanotubes under ambient pressure and moderate temperatures. Science 285:91

Chen B, Li B, Chen L (2008) Prompted hydrogenation of carbon nanotubes by doping light metals. Appl Phys Lett 93:043104

Choi S-M, Jhi SH (2009) Electronic property of Na-doped epitaxial graphenes on SiC. Appl Phys Lett 94:153108

Ci L, Song L, Jin C, Jariwala D, Wu D, Li Y, Srivastava A, Wang ZF, Storr K, Balicas L, Liu F, Ajayan PM (2010) Atomic layers of hybridized boron nitride and graphene domains. Nat Mater 9:430

Dai J, Yuan J, Giannozzi P (2009) Gas adsorption graphene doped with B, N, Al, and S: a theoretical study. Appl Phys Lett 95:232105

Ding J, Qiao Z, Feng W, Yao Y, Niu Q (2011) Engineering quantum anomalous/valley Hall states in graphene via metal-atom adsorption: an ab-initio study. Phys Rev B 84:195444

Duren T, Sarkisov L, Yaghi OM, Snurr RQ (2004) Design of new materials for methane storage. Langmuir 20:2683

Durgun E, Ciraci S, Yildirim T (2008) Functionalization of carbon-based nanostructures with light transition-metal atoms for hydrogen storage. Phys Rev B 77:085405

Esquinazi P, Spemann D, Höhne R, Setzer A, Han K-H, Butz T (2003) Induced Magnetic Ordering by Proton Irradiation in Graphite Phys. Rev Lett 91:227201

Geim AK, Novoselov KS (2007) The rise of Graphene. Nat Mater 6:183

Geim AK (2009) Graphene: status and prospects. Science 324:1530

Giannozzi P et al (2009) QUANTUM ESPRESSO: a modular and open-source software project for quantum simulations of materials. J Phys Condens Matter 21:395502

Hohenberg P, Kohn W (1964) Inhomogeneous electron gas. Phys Rev 136:B864

Johll H, Kang HC, Tok ES (2009) Density functional theory study of Fe Co, and Ni adatoms and dimers adsorbed on graphene. Phys Rev B 79:245416

Kaloni TP, Upadhyay Kahaly M, Cheng YC, Schwingenschlögl U (2008) K-intercalated carbon systems: effects of dimensionality and substrate. EPL 98:67003

Kaloni TP, Upadhyay Kahaly M (2011) Induced magnetism in transition metal intercalated graphitic systems. J Mater Chem 21:18681

Kaloni TP, Cheng YC, Schwingenschlögl U (2012) Fluorinated monovacancies in graphene: even–odd effect. EPL 100:37003

Kaloni TP, Upadhyay Kahaly M, Faccio R, Schwingenschlögl U (2013) Modelling magnetism of C at O and B monovacancies in graphene. Carbon 64:281

Kaloni TP, Balatsky AV, Schwingenschlögl U (2013) Substrate-enhanced superconductivity in Li-decorated graphene. EPL 104:47013

Kaloni TP, Joshi RP, Adhikari NP, Schwingenschlögl U (2014) Band gap tunning in BN-doped graphene systems with high carrier mobility. Appl Phys Lett 104:073116

Karki DB, Adhikari NP (2014) First-principles study of the stability of graphene and adsorption of halogen atoms (F, Cl and Br) on hydrogen passivated graphene Int. J Mod Phys B 28:1450141

Klimes J, Michaelides A (2012) Perspective: advances and challenges in treating van der Waals dispersion forces in density functional theory. J Chem Phys 137: 120901

Kohn W, Sahm LJ (1965) Self-consistent equations including exchange and correlation effects. Phys Rev 140:1133

Kwon YK (2010) Hydrogen adsorption on sp2-bonded carbon structures: Ab-initio study. J Korean Phys Soc 57:778

Lamichhane S, Pantha N, Adhikari NP (2014) Hydrogen storage on platinum decorated graphene: a first-principles study. Bibechana 11(1):107

Liu X, Wang CZ, Yao YX, Lu WC, Tringides MC, Ho KH (2011) Bonding and charge transfer by metal adatom adsorption on graphene. Phys Rev B 83:235411

Ma S, Sun D, Simmons JM, Collier CD, Yuan D, Zhou HC (2008) Metal-organic framework from an anthracene derivative containing nanoscopic cages exhibiting high methane uptake. J Am Chem Soc 130:1012

Marzari N, Vanderbilt D, de Vita A, Payne MC (1999) Thermal contraction and disordering of the Al(110) surface. Phys Rev lett 82:3296

Medeiros VCP, de Mota FN, Mascarenhas JSA, de Castilho CMC (2010) Adsorption of monovalent metal atoms on graphene: a theoretical approach. Nanotechnology 21:115701

Mukherjee S, Kaloni TPJ (2012) Electronic properties of boron-and nitrogen-doped graphene: a first principles study. Nanopart Res 14:1059

Nakanishi E, Reid RC (1971) Liquid natural gas–water reactions. Chem Eng Prog 67:36

Novoselov KS, Jiang Z, Zhang Y, Morozov SV, Stormer HL, Zeitler U, Maan JC, Boebinger GS, Kim P, Geim AK (2007) Room-temperature quantum hall effect in graphene. Science 315:1379

Novoselov KS, Geim AK, Morozov SV, Jiang D, Katsnelson MI, Dubonos SV, Grigorieva IV, Firsov AA (2004) Electric field effect in atomically thin carbon films. Science 306:666

Novoselov KS, Geim AK, Morozov SV, Jiang D, Katsnelson MI, Zhang Y, Grigorieva IV, Dubonos SV, Firsov AA (2005) Two-dimensional gas of massless Dirac fermions in graphene. Nature 438:197

Oli BD, Bhattarai C, Nepal B, Adhikari NP (2013) First-Principles study of adsorption of alkali metals (Li, Na, K) on graphene. Adv Nanomater Nanotechnol 143:515

Orimo S, Nakamori Y, Eliseo JR, Zttel A, Jensen CM (2007) Complex hydrides for hydrogen storage. Chem Rev 107:4111

Palacios JJ, Rossier JF, Brey L (2008) Vacancy-induced magnetism in graphene and graphene ribbons. Phys Rev B 77:195428

Pan L, Sander MB, Huang X, Li J, Smith M, Bittner E, Bockrath B, Johnson JK (2008) Microporous metal organic materials: promising candidates as sorbents for hydrogen storage. J Am Chem Soc 126:1308

Park CH, Louie SG (2010) Tunable excitons in biased bilayer graphene. Nano Lett 10:426

Perdew JP, Burke K, Ernzerhof M (1996) Generalized gradient approximation made simple. Phys Rev 77:3865

Pumera M (2011) Graphene-based nanomaterials for energy storage. Energy Environ Sci 4:668

Quantum ESPRESSO user manual, version 4.3.1

Saha SK, Chandrakanth RC, Krishnamurthy HR, Waghmare UV (2009) Mechanisms of molecular doping of graphene: a first-principles study. Phys Rev B 80:155414

Singh N, Kaloni TP, Schwingenschlögl U (2013) Additional information on Appl. Phys Lett Appl Phys Lett 102:023101

Thapa R, Sen D, Mitra MK, Chattopadhyay KK (2011) Palladium atoms and its dimers adsorbed on graphene: first-principles study. Phys B Condens Matt 406:368

Ugeda MM, Brihuega I, Guinea F, Gómez-Rodríguez JM (2010) Missing atom as a source of carbon magnetism. Phys Rev Lett 104:096804

Ulman K, Bhaumik D, Wood BC, Narasimhan S (2014) Physical origins of weak H2 binding on carbon nanostructures: insight from ab initio studies of chemically functionalized graphene nanoribbons. J Chem Phys 140:174708

Valencia F, Romero A, Ancilotto F, Silvestrelli P (2006) Lithium adsorption on graphite from density functional theory calculations. J Phys Chem B 110:14832

Wallace PR (1947) The band theory of graphite. Phys Rev 71:622

Wood BC, Bhide SY, Dutta D, Kandagal VS, Pathak AD, Punnathanam SN, Aayappa KG, Narasimhan S (2012) Methane and carbon dioxide adsorption on edge-functionalized graphene: a comparative DFT study. J Chem Phys 137:054702

Wu BR, Yang CK (2012) Electronic structures of graphane with vacancies and graphene adsorbed with fluorine atoms. AIP Adv 2:012173

Zhou JG, Willians QL (2011) Hydrogen storage on platinum decorated carbon nanotubes with boron, nitrogen dopants or sidewall vacancies. J Nano Res 15, 29. http://arxiv.org/pdf/1104.3174v1.pdf

Zhou M, Lu Y, Zhang C, Feng YP (2010) Strain effects on hydrogen storage capability of metal-decorated graphene: a first-principles study. Appl Phys Lett 97:103109